Highly selective Fe^{3+} sensing and proton conduction in a water-stable sulfonate-carboxylate Tb-organic-framework

Xi-Yan Dong,[a,b] Rui Wang,[a] Jun-Zhe Wang,[a] Shuang-Quan Zang,*[a] and Thomas C. W. Mak[a,c]

[a] College of Chemistry and Molecular Engineering, Zhengzhou University, Zhengzhou 450001, China

[b] School of Physics and Chemistry, Henan Polytechnic University, Jiaozuo 454000, China

[c] Department of Chemistry and Center of Novel Functional Molecules, The Chinese University of Hong Kong, Shatin, New Territories, Hong Kong SAR, China

Author for correspondence: **Dr. S.-Q. Zang**

Supporting Information

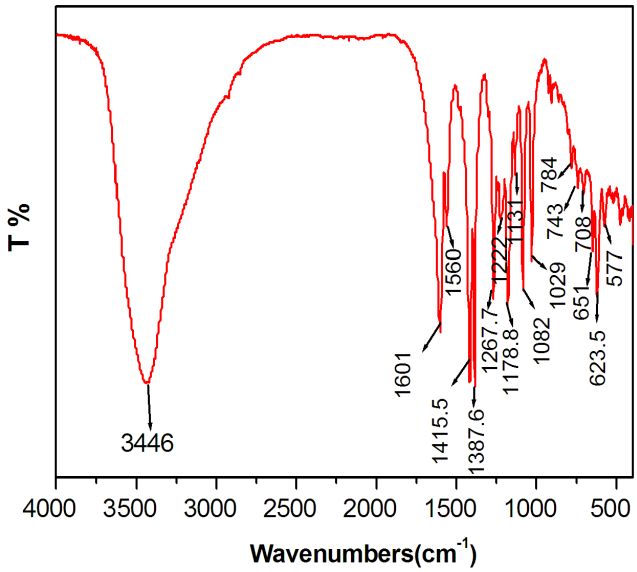

Fig.S1 IR spectrum of **Tb-DSOA** at room temperature.

Table S1. Crystal data and structure refinement for **Tb-DSOA**

Temperature	293(2) K
Formula	C14 H24 O21 S2 Tb2
Formula weight	910.29
Crystal system	tetragonal
Space Group	I-4
Z	4
a (Å)	12.8897(5)
b (Å)	12.8897(5)
c (Å)	16.4462(12)
V (Å^3)	2732.4(2)
ρ_{calcd} (g cm^{-3})	2.213
θ range (°)	3.16 - 24.99
F(000)	1752
μ (mm^{-1})	5.376
Refln.collected	3164
Independent reflections	2254
Completeness	99.8 %
Refinement Method	Full-matrix least-squares on F^2
Data / restraints / parameters	2254 / 30 / 182
R(int)	0.0238
GOF	1.016
^{a} $R_1[I > 2\sigma(I)]$, wR_2	0.0265, 0.0503

R_1[all data] , wR_2	0.0277, 0.0513

[a] $R_1=\Sigma||F_o| - |F_c||/\Sigma|F_o|$, $wR_2=[\Sigma[w(F_o^2 - F_c^2)^2]/\Sigma w(F_o^2)^2]^{1/2}$

Table S2. Selected bond lengths (Å) and bond angles (°) for **Tb-DSOA**

	Bond lengths (Å)		
Tb(1)–O(1)#1	2.316(5)	Tb(1)–O(7)#4	2.451(4)
Tb(1)–O(2)#2	2.336(5)	Tb(1)–O(2W)	2.505(5)
Tb(1)–O(7)	2.354(4)	Tb(1)–Tb(1)#5	3.7826(5)
Tb(1)–O(6)	2.363(5)	Tb(1)–Tb(1)#3	3.7826(5)
Tb(1)–O(7)#3	2.391(4)	Tb(1)–Tb(1)#4	3.9974(6)
Tb(1)–O(1W)	2.428(5)		
	Bond Angles (°)		
O(1)#1–Tb(1)–O(2)#2	100.27(2)	O(1)#1–Tb(1)–Tb(1)#5	121.76(1)
O(1)#1–Tb(1)–O(7)	142.49(2)	O(2)#2–Tb(1)–Tb(1)#5	72.26(1)
O(2)#2–Tb(1)–O(7)	98.48(2)	O(7)–Tb(1)–Tb(1)#5	37.48(1)
O(1)#1–Tb(1)–O(6)	80.77(2)	O(6)–Tb(1)–Tb(1)#5	141.91(1)
O(2)#2–Tb(1)–O(6)	138.38(2)	O(7)#3–Tb(1)–Tb(1)#5	39.21(1)
O(7)–Tb(1)–O(6)	105.48(2)	O(1W)–Tb(1)–Tb(1)#5	96.34(2)
O(1)#1–Tb(1)–O(7)#3	82.67(2)	O(7)#4–Tb(1)–Tb(1)#5	77.26(1)
O(2)#2–Tb(1)–O(7)#3	73.92(2)	O(2W)–Tb(1)–Tb(1)#5	139.03(1)
O(7)–Tb(1)–O(7)#3	71.75(2)	O(1)#1–Tb(1)–Tb(1)#3	65.04(1)
O(6)–Tb(1)–O(7)#3	145.94(2)	O(2)#2–Tb(1)–Tb(1)#3	108.70(2)
O(1)#1–Tb(1)–O(1W)	138.8(2)	O(2)#2–Tb(1)–Tb(1)#3	78.26(1)
O(2)#2–Tb(1)–O(1W)	75.3(2)	O(6)–Tb(1)–Tb(1)#3	109.17(1)
O(7)–Tb(1)–O(1W)	77.52(2)	O(7)#3–Tb(1)–Tb(1)#3	36.81(1)
O(6)–Tb(1)–O(1W)	77.28(2)	O(1W)–Tb(1)–Tb(1)#3	155.78(1)
O(7)#3–Tb(1)–O(1W)	132.07(2)	O(7)#4–Tb(1)–Tb(1)#3	38.06(1)
O(1)#1–Tb(1)–O(7)#4	79.48(2)	O(2W)–Tb(1)–Tb(1)#3	130.85(1)
O(2)#2–Tb(1)–O(7)#4	143.76(2)	Tb(1)#5–Tb(1)–Tb(1)#3	63.79(4)
O(7)–Tb(1)–O(7)#4	66.38(2)	O(1)#1–Tb(1)–Tb(1)#4	112.35(1)
O(6)–Tb(1)–O(7)#4	77.72(1)	O(2)#2–Tb(1)–Tb(1)#4	129.55(1)
O(7)#3–Tb(1)–O(7)#4	70.09(2)	O(7)–Tb(1)–Tb(1)#4	34.50(9)
O(1W)–Tb(1)–O(7)#4	127.92(2)	O(6)–Tb(1)–Tb(1)#4	85.77(1)
O(1)#1–Tb(1)–O(2W)	67.86(2)	O(7)#3–Tb(1)–Tb(1)#4	73.38(9)
O(2)#2–Tb(1)–O(2W)	66.78(2)	O(1W)–Tb(1)–Tb(1)#4	100.34(1)
O(7)–Tb(1)–O(2W)	149.63(2)	O(7)#4–Tb(1)–Tb(1)#4	32.96(9)
O(6)–Tb(1)–O(2W)	75.65(2)	O(2W)–Tb(1)–Tb(1)#4	161.22(1)
O(7)#3–Tb(1)–O(2W)	124.27(2)	Tb(1)#5–Tb(1)–Tb(1)#4	58.10(3)
O(1W)–Tb(1)–O(2W)	73.13(2)	Tb(1)#3–Tb(1)–Tb(1)#4	58.10(3)
O(7)#4–Tb(1)–O(2W)	140.46(2)		

Symmetry transformations used to generate equivalent atoms: #1 = $y - 1/2, -x + 1, -z + 3/2$; #2 = $-x + 1/2, -y + 3/2, z + 1/2$; #3 = $-y + 1, x, -z + 2$; #4 = $-x+1, -y + 1, z$; #5 = $y, -x +1, -z +2$.

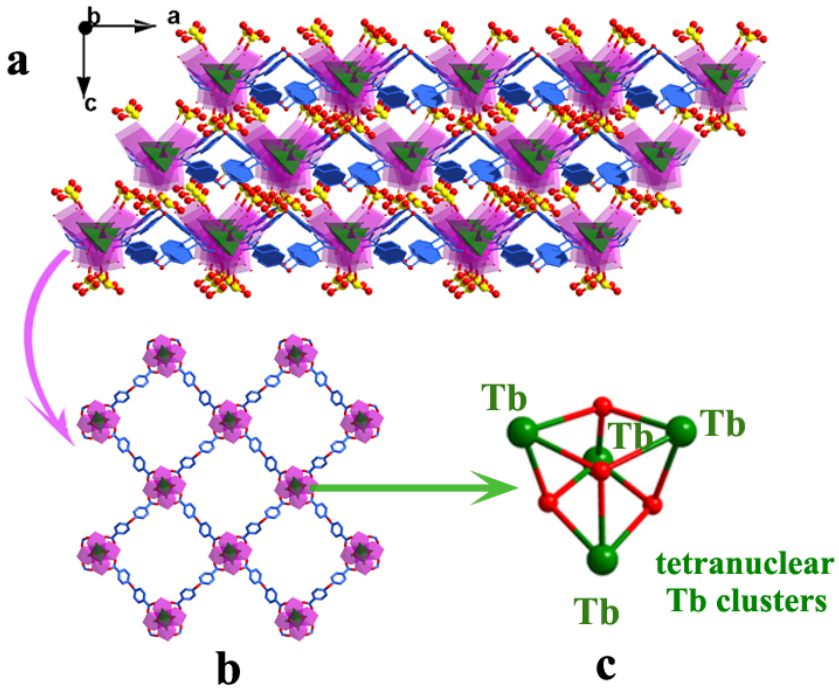

Fig. S2 (a) View of 3D structure of **Tb-DSOA** down the *b*-axis; The sulfonate groups of $DSOA^{4-}$ ligands bridge the adjacent grid plane through the Tb–O bond (one oxygen of sulfonate group) to give rise to a 3D-network; (b) 2D sheet-like grid plane built from $[Tb_4(\mu_3\text{-}OH)_4]$ clusters linked by the carboxylate groups of the $DSOA^{4-}$ ligands; (c) Tetranuclear Tb clusters (H atoms of hydroxyl are omitted).

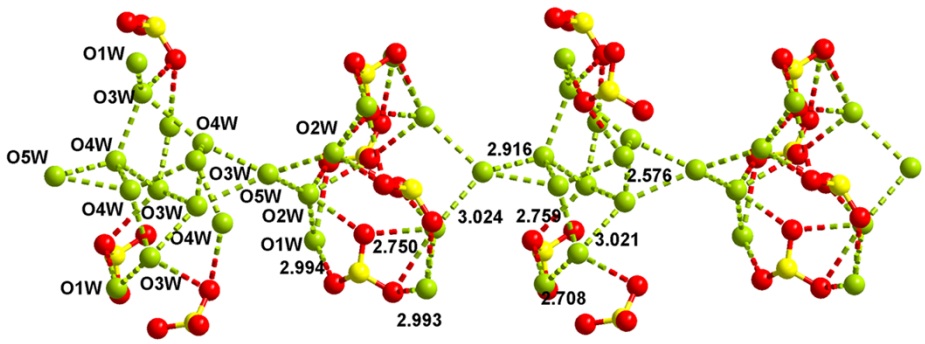

Fig. S3 H-bond association as potential pathway involving uncoordinated sulfonate oxygen atoms (red), oxygen of aqua ligands and solvent water molecules (green).

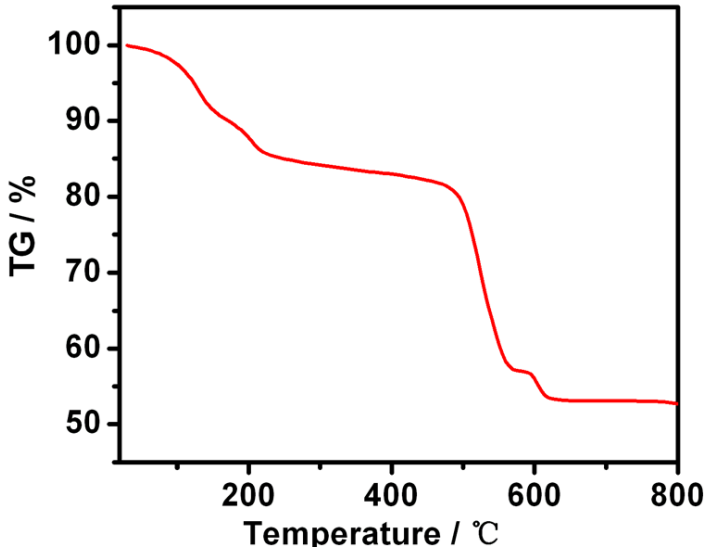

Fig. S4 TG plot of as prepared **Tb-DSOA**.

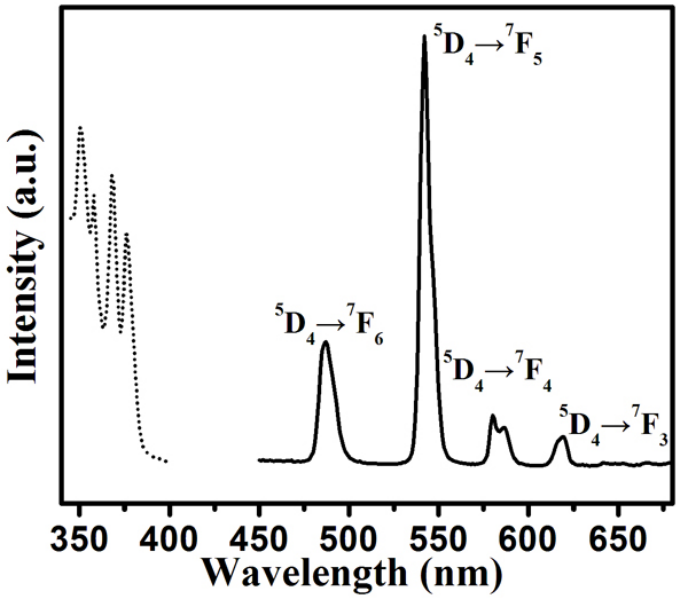

Fig. S5 Excitation (dotted line, λ_{em} = 542 nm) and emission spectra (solid line, λ_{ex} = 350 nm) of pure **Tb-DSOA** solid samples with 2nm slit widths.

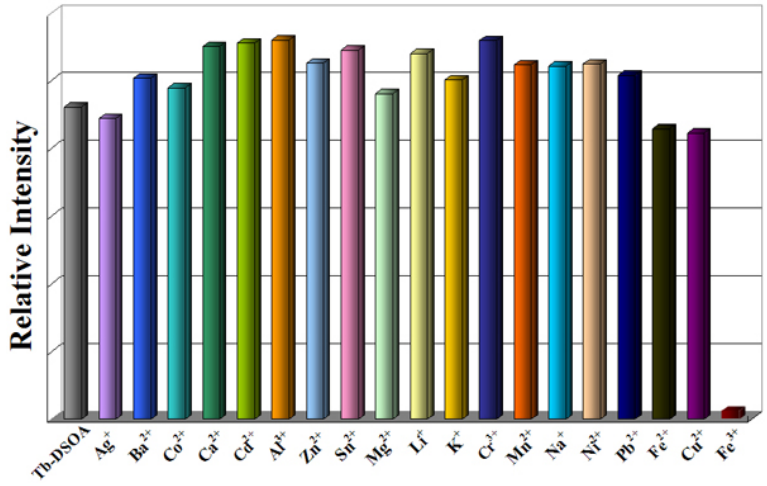

Fig. S6 Histogram Comparison of the photoluminescence intensity of the $^5D_4 \rightarrow {}^7F_5$ transition (542nm) of M^{n+}@Tb-DSOA after immersion in 0.01M M^{n+} aqueous solution for one day. (M = Na^+, K^+, Li^+, Ag^+, Mg^{2+}, Ba^{2+}, Ca^{2+}, Pb^{2+}, Sn^{2+}, Cu^{2+}, Fe^{2+}, Co^{2+}, Ni^{2+}, Cd^{2+}, Zn^{2+}, Mn^{2+}, Al^{3+}, Cr^{3+}, Fe^{3+} respectively) monitored at 350 nm.

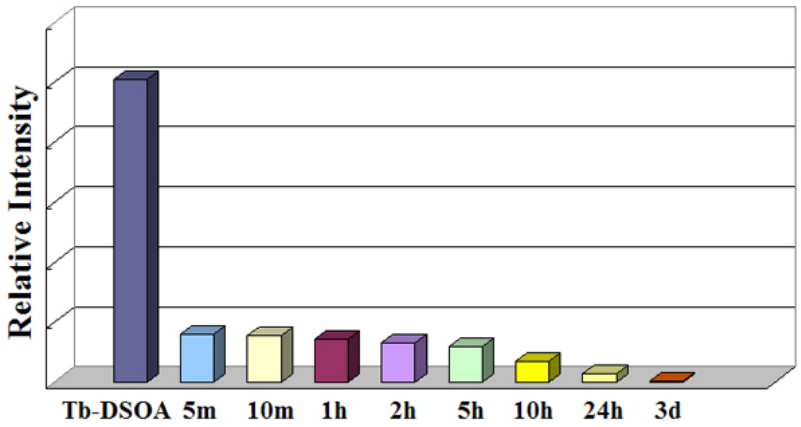

Fig. S7 The emission intensity histogram of $^5D_4 \rightarrow {}^7F_5$ transition (542nm) of time-dependent Fe^{3+}@Tb-DSOA obtained after immersion in 0.01 M Fe^{3+} aqueous solution for different time.

Table S3. The ICP results of Fe^{3+}@Tb-DSOA after different immersion time.

Immersion Time	5 min	10 min	30 min	1 h	2 h	5 h	10 h	24 h
Fe/ Tb	1:15.56	1:15.48	1:14.13	1:12.35	1:11.61	1:8.62	1:7.64	1:5.64

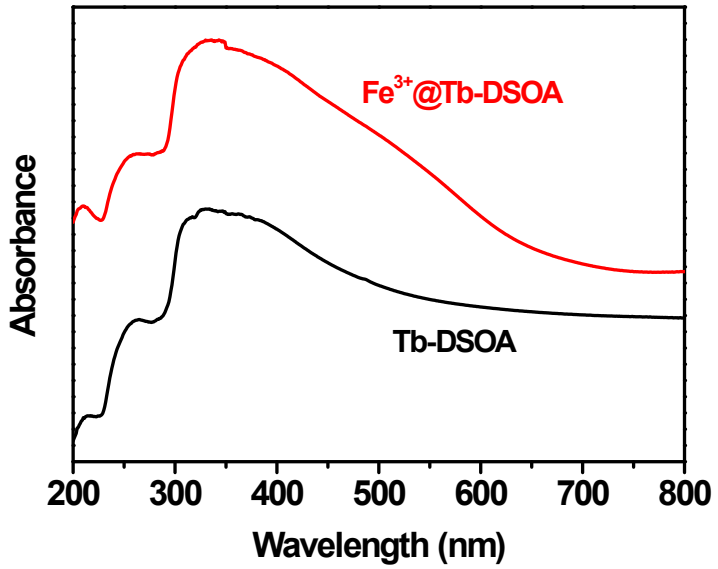

Fig. S8 The diffuse reflectance ultraviolet-visible (DR UV–vis) spectra of solid samples of Tb-DSOA and Fe^{3+}@Tb-DSOA treated with 0.01 mol L^{-1} $Fe(NO_3)_3$ aqueous solution for 24 h.

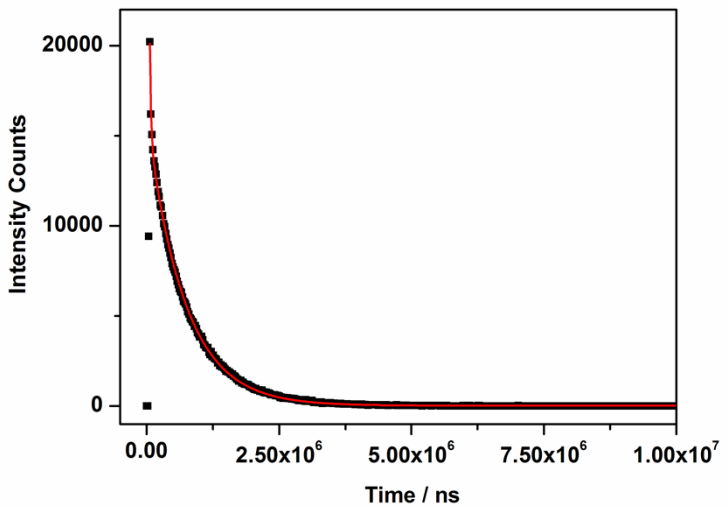

Fig. S9 The emission decay curve of **Tb-DSOA** (λ_{ex} = 350nm, λ_{em} =542 nm) at 298 K.

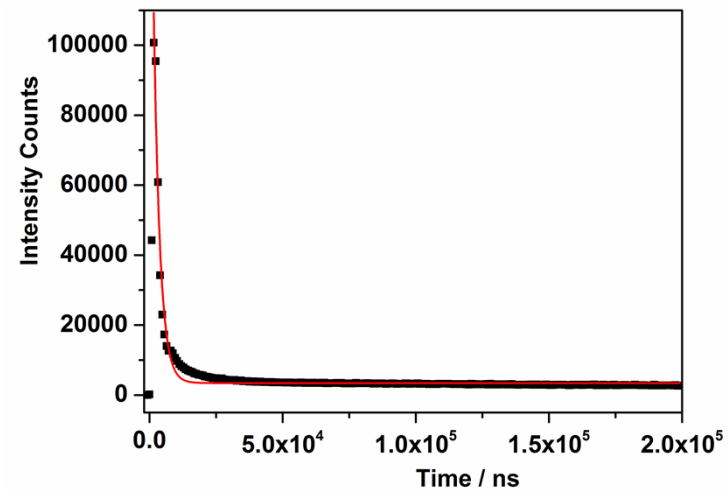

Fig. S10 The emission decay curve of Fe^{3+}@Tb-DSOA (λ_{ex} = 350nm, λ_{em} =542 nm) at 298 K.

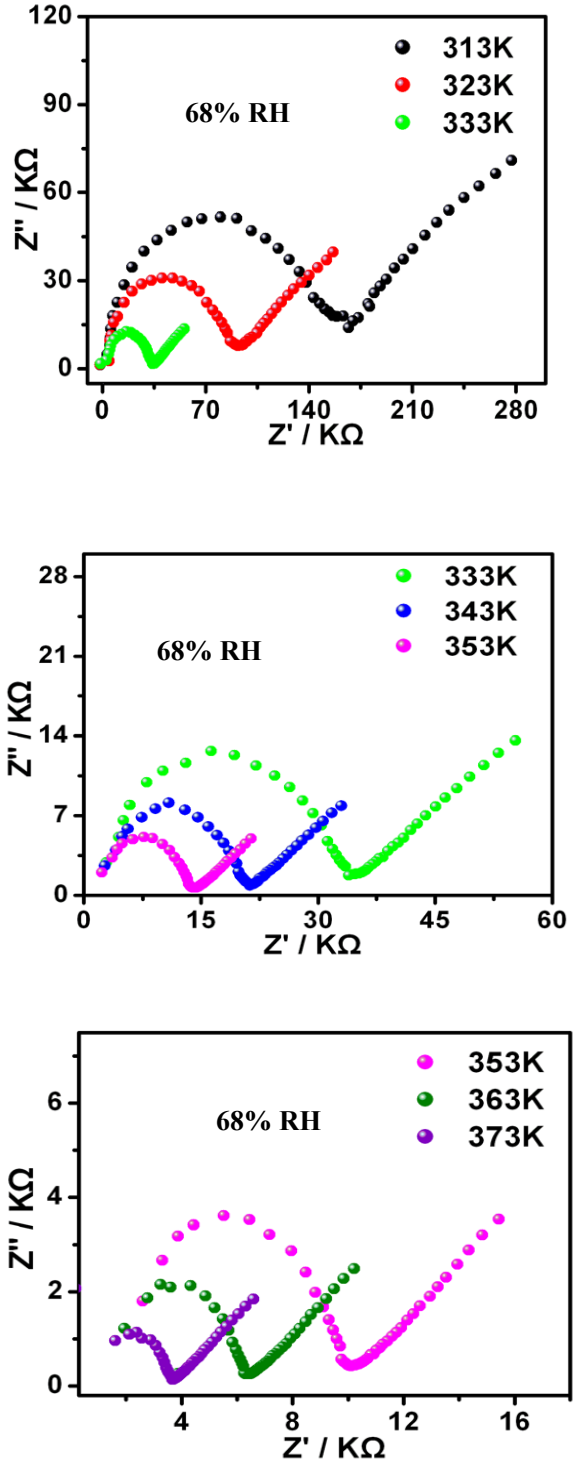

Fig. S11 The Nyquist plots for **Tb-DSOA** at 68% relative humidity at different temperatures.

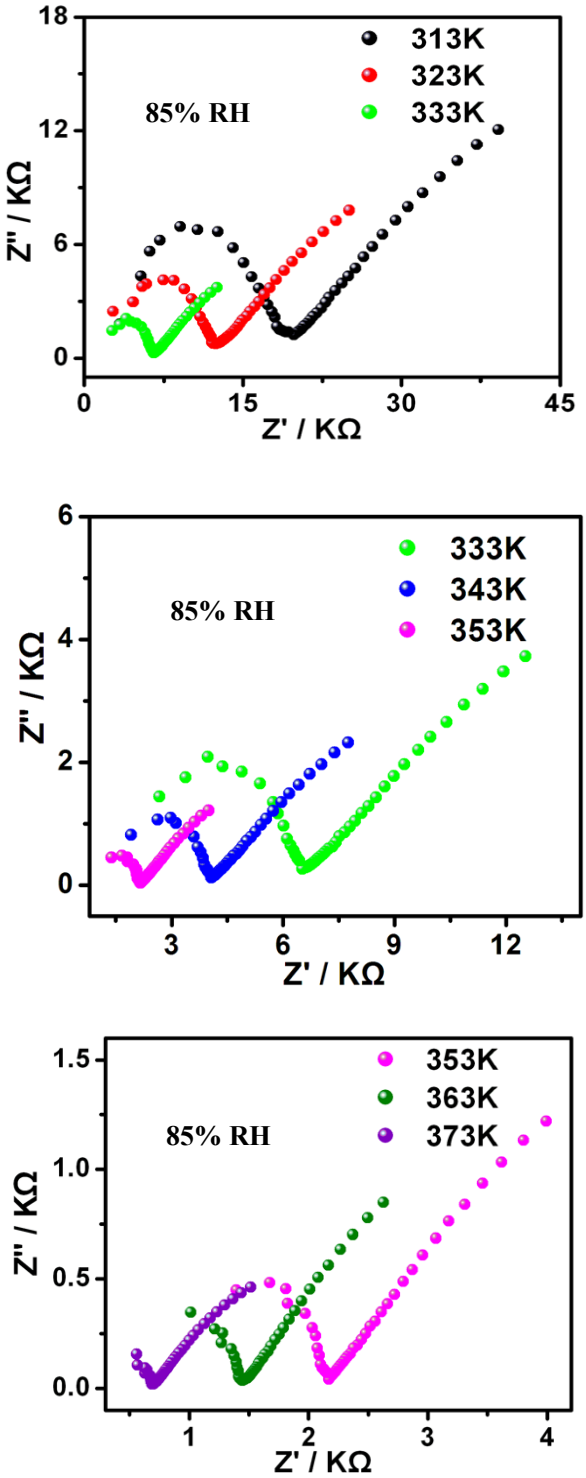

Fig. S12 The Nyquist plots for **Tb-DSOA** at 85% relative humidity at different temperatures.

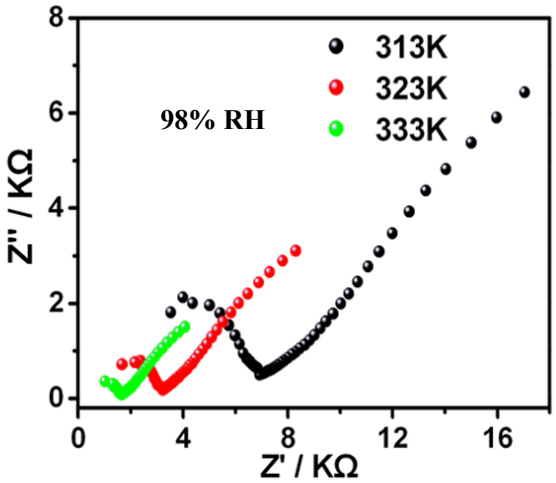

Fig. S13 The Nyquist plots for **Tb-DSOA** at 98% relative humidity in the range of 313–333 K.

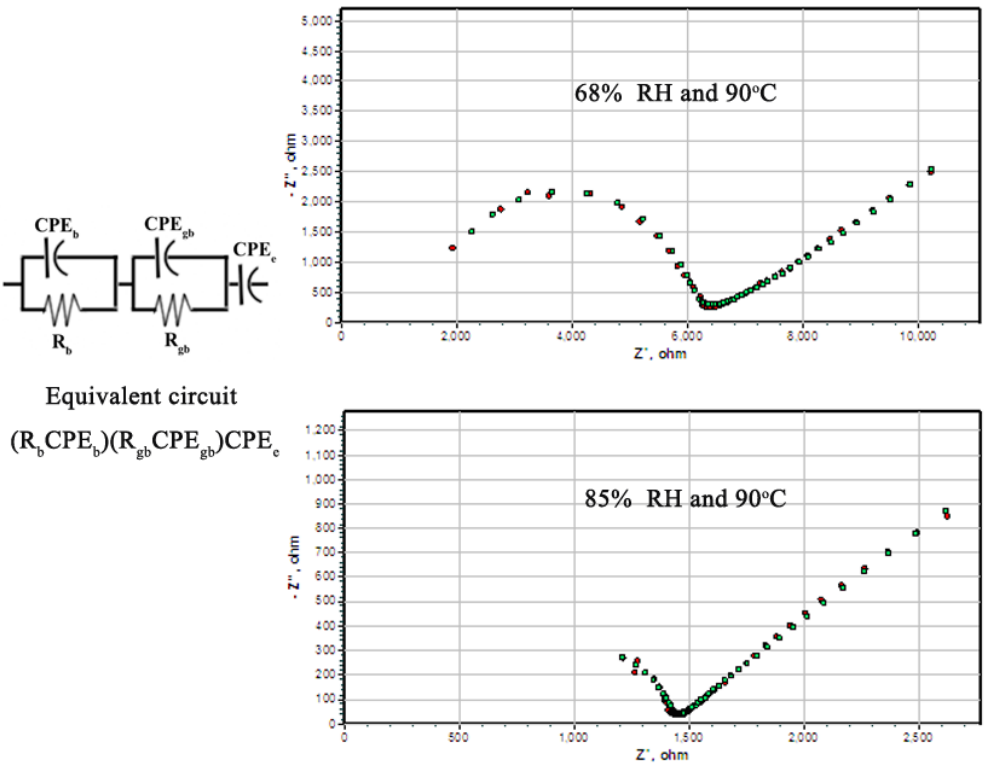

Fig. S14 The representative measured Nyquist plots (Red circle) and the fits of impedance data to the equivalent circuit of $CPE_e(R_bCPE_b)(R_{gb}CPE_{gb})$ (green square). (where R_b and R_{gb} is the resistance of proton transfer in the bulk phase and grain boundary, respectively; CPE_b and CPE_{gb} are the constant-phase element in the bulk phase and grain boundary, respectively.)

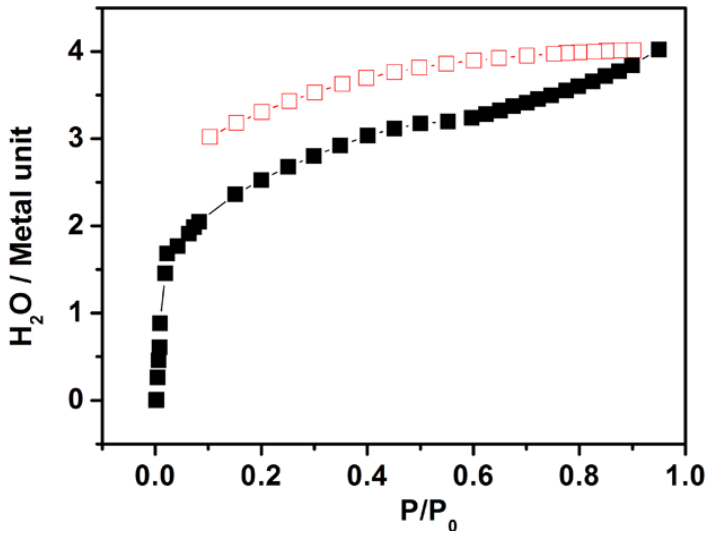

Fig. S15 Water vapor adsorption/desorption isotherms of **Tb-DSOA**. Filled and open symbols correspond to adsorption and desorption, respectively.

Table S4: Compare proton conductivity of **Tb-DSOA** in this work with that of some CPs or MOFs containing sulfonate groups or sulfone groups, hybrid acid@MOFs as well as Nafion.

Compound	Ligand	Prominent features / guest	σ / S cm^{-1}	RH %	T (°C)
Tb-DSOA	disodium-2,2′-disulfonate-4,4'-oxydibenzoic acid	non-coordinating sulfonate oxygen atoms, aqua ligands line channels / lattice water	2.3×10^{-7}	43	100
			4.0×10^{-7}	53	100
			1.7×10^{-4}	98	100
β-PCMOF2[1]	trisodium 2,4,6-trihydroxy-1,3,5-trisulfonate benzene	Oxygen atoms from SO_3^- groups line channels / lattice water	1.8×10^{-6}	50	85
			1.3×10^{-3}	90	85
PCMOF2$_{1/2}$[1]	trisodium 2,4,6-trihydroxy-1,3,5-trisulfonate benzene and 1,3,5-benzenetriphosphonic acid	Oxygen atoms from SO_3^-, PO_3^{2-} groups line channels / lattice water	2.4×10^{-5}	50	85
			2.1×10^{-2}	90	85
PCMOF-3[2]	1,3,5-benzenetriphosphonate	Aqua ligands and phosphonate oxygen atoms line interlayer/ lattice water	4.5×10^{-8}	44	25
			3.5×10^{-5}	98	25
Zn(5-sipH)-(bpy)]·DMF ·2H$_2$O[3]	5-sulfoisophthalic acid and 4,4′-bipyridine	non-coordinating sulfonic acid groups on the pore surface / DMF and water	3.9×10^{-4}	60	25

$[Zn(H_2O)(5\text{-sipH})\text{-}(bpe)_{0.5}]\cdot DMF$[3]	5-sulfoisophthalic acid and 1,2-di(4-pyridyl)ethyrene	non-coordinating sulfonic acid groups on the pore surface / DMF	3.4×10^{-8}	60	25
$[Zn_3(5\text{-sip})_2(5\text{-sipH})(bpy)]\cdot(DMF)\cdot2(DMA)$[3]	5-sulfoisophthalic acid and 4,4′-bipyridine	non-coordinating sulfonic acid groups on the pore surface / DMF and DMA	8.7×10^{-5}	60	25
Cu-DSOA[4]	disodium-2,2′-disulfonate-4,4'-oxydibenzoic acid	non-coordinating sulfonate oxygen atoms line channels / hydroniums	1.9×10^{-3}	98	85
Sr-SBBA[5]	4,4′-sulfobisbenzoic acid	Sulfone group in backbone facilitate H-bonding	4.4×10^{-5}	98	25
$[H_3O][Mn_3(\mu_3\text{-}OH)(C_{14}H_8O_6S)_3(H_2O)](DMF)$[6]	4,4′-sulfonyldibenzoic acid	hydrogen bonded guests /hydronium ion, DMF and H_2O	3×10^{-4}	98	34
$\{Fe(ox)(H_2O)_2\}$[7]	Oxalic acid	Water molecules coordinate axially to ferrous ions and form a 1D ordered array of	1.3×10^{-3}	98	25
H_2SO_4@MIL-101[8]	Hybrid composite	Inorganic acids inside pores of Cr-MIL-101 / H_2SO_4	6×10^{-2}	20	80
TfOH@MIL-101[9]	Hybrid composite	organic acids inside pores of / trifluoromethanesulfonic acid	8×10^{-2}	15	60
Nafion[10]	Polymer namely perfluorosulfonic membranes	–	10^{-2}	98	20-80

References:

1. S. R. Kim, K. W. Dawson, B. S. Gelfand, J. M. Taylor and G. K. H. Shimizu, *J. Am. Chem. Soc.*, 2013, **135**, 963−966.
2. J. M. Taylor, R. K. Mah, I. L. Moudrakovski, C. I. Ratcliffe, R. Vaidhyanathan and G. K. H. Shimizu, *J. Am. Chem. Soc.*, 2010, **132,** 14055–14057.
3. P. Ramaswamy, R. Matsuda, W. Kosaka, G. Akiyama, H. J. Jeon and S. Kitagawa, *Chem. Commun.*, 2014, **50**, 1144–1146.
4. X.-Y. Dong, R. Wang, J.-B. Li, S.-Q. Zang, H.-W. Hou and T. C. W. Mak, *Chem. Commun.,* 2013, **49**, 10590 –10592.
5. T. Kundu, S. C. Sahoo and R. Banerjee, *Chem. Commun.*, 2012, **48**, 4998–5000.
6. S. Bhattacharya, M. Gnanavel, A. J. Bhattacharyya and S. Natarajan, *Cryst. Growth Des.*, 2014, **14**, 310–325.

7. T. Yamada, M. Sadakiyo and H. Kitagawa, *J. Am. Chem. Soc.*, 2009, **131**, 3144–3145.
8. V. G. Ponomareva, K. A. Kovalenko, A. P. Chupakhin, D. N. Dybtsev, E. S. Shutova and V. P. Fedin, *J. Am. Chem. Soc.*, 2012, **134**, 15640–15643.
9. D. N. Dybtsev, V. G. Ponomareva, S. B. Aliev, A. P. Chupakhin, M. R. Gallyamov, N. K. Moroz, B. A. Kolesov, K. A. Kovalenko, E. S. Shutova and Vladimir P. Fedin, *ACS Appl. Mater. Interfaces,* 2014, **6**, 5161−5167.
10. M. Yoon, K. Suh, S. Natarajan and K. Kim, *Angew. Chem. Int. Ed.*, 2013, **52**, 2688−2700.